Colloids and Surfaces B: Biointerfaces
April 2021, Volume 200, Pages 111561 (8p.)
https://doi.org/10.1016/j.colsurfb.2021.111561
https://archimer.ifremer.fr/doc/00667/77875/

In vitro evaluation of polymeric nanoparticles with a fluorine core for drug delivery triggered by focused ultrasound

Somaglino Lucie [1, 2], Mousnier L [3], Giron A [1], Urbach W [1, 4], Tsapis N [3], Taulier N [1, *]

[1] Sorbonne Université, CNRS, INSERM, Laboratoire d'Imagerie Biomédicale, LIB, F-75006 Paris, France
[2] IFREMER, La Seyne-sur-Mer, France
[3] Université Paris-Saclay, CNRS, Institut Galien Paris Saclay, 92296, Châtenay-Malabry, France
[4] Laboratoire de Physique de l'École Normale Supérieure, ENS, Université PSL, CNRS, Sorbonne Université, Université de Paris, F-75005 Paris, France

* Corresponding author : N. Taulier, email address : nicolas.taulier@sorbonne-universite.fr

Abstract :

Polymeric nanoparticles are being intensively investigated as drug carriers. Their efficiency could be enhanced if the drug release can be triggered using an external stimulus such as ultrasound. This approach is possible using current commercial apparatus that combine focused ultrasound with MRI to perform ultrasonic surgery. In this approach, nanoparticles made of a perfluoro-octyl bromide core and a thick polymeric (PLGA-PEG) shell may represent suitable drug carriers. Indeed, their perfluorocarbon core are detectable by 19F MRI, while their polymeric shell can encapsulate drugs. However, their applicability in ultrasound-triggered drug delivery remains to be proven. To do so, we used Nile red as a model drug and we measured its release from the polymeric shell by spectrofluorometry. In the absence of ultrasound, only a small amount of Nile red release was measured (<5%). Insonations were performed in a controlled environment using a 1.1 MHz transducer emitting tone bursts for a few minutes, whereas a focused broadband hydrophone was used to detect the occurrence of cavitation. In the absence of detectable inertial cavitation, less than 5% of Nile red was released. In the presence of detectable inertial cavitation, Nile red release was ranging from 10 to 100%, depending of the duty cycle, acoustic pressure, and tank temperature (25 or 37°C). Highest releases were obtained only for duty cycles of 25% at 37°C and 50% at 25°C and for a peak-to-peak acoustic pressure above 12.7 MPa. Electron microscopy and light scattering measurements showed a slight modification in the nanoparticle morphology only at high release contents. The occurrence of strong inertial cavitation is thus a prerequisite to induce drug release for these nanoparticles. Since strong inertial cavitation can lead to many unwanted biological effects, these nanoparticles may not be suitable for a therapeutic application using ultrasound-triggered drug delivery.

Highlights

► Nanoparticles made of a PFOB core and a thick PLGA-PEG shell ► Ultrasound-triggered release of Nile red encapsulated into the PLGA-PEG shell ► In the absence of detectable inertial cavitation, release is <5% ► In the presence of detectable inertial cavitation, release ranges from 10 to 100% ► Release over 30% occurs only if both duty cycle & acoustic pressure are high enough

Keywords : ultrasound, drug delivery, nanoparticles, PFOB, cavitation

1. Introduction

Although nanomedicines have exhibited promising preclinical efficacy to treat cancer, only a few have reached the market until now.[1] Among clinically approved nanomedicines, one can cite PEGylated liposomal doxorubicin (Doxil® / Caelyx®). It did not improve the overall survival in breast cancer but it is a major evolution in the treatment of Kaposi sarcoma.[2, 3] Many nanomedicines that have been developed for cancer treatments rely on the so-called enhanced permeation and retention effect (EPR), which facilitates the escape of nanomedicines through leaky solid tumor vasculature and retention due to reduced lymphatic drainage.[4, 5, 6] Thanks to the EPR effect, tumor passive targeting via nanomedicine can be achieved and the drug concentration in the tumor is enhanced compared to a free drug, leading to an enhanced efficiency.[7] But the proportion of nanomedicines usually reaching the tumor site is below 10% of the injected dose.[8] In addition, if tumor models implanted in mice almost systematically exhibit an EPR effect, this is far to be the case for patient tumors.[9] To overcome the unreliability of the presence of the EPR effect in patients, stimulus-sensitive systems have been developed.[10] The local application of the stimulus allows to trigger the drug release in the vicinity of the solid tumor and therefore increase drug concentration therein. Stimuli can be exogenous[11] such as magnetic field, temperature, ultrasound, light or electric pulses; or endogenous[12] such as intracellular enzymes, pH or redox gradients. Ultrasound represents an attractive technique as it is widely available in hospitals through echographs and is easily manipulated.[13] In addition, commercial apparatus using the MRI-guided high intensity focused ultrasound (MRI-g-HIFU) technique are currently used in clinics for the treatment of fibroids,[14] and in ongoing clinical trials for the treatment of breast, liver, prostate, and brain cancer.[15]

*Corresponding author
Email address: nicolas.taulier@sorbonne-universite.fr (N. Taulier)

Most carriers under development for ultrasound triggered delivery are liposomes encapsulating a cytotoxic drug, mostly doxorubicin [16, 17, 18, 19] as liposomal doxorubicin formulations have already been approved by several major drug agencies, including Federal Drug Agency (FDA) and European Medicines Agency (EMA), and are currently commercialized (Myocet® and Doxil®/Caelyx®). For example, Thermodox®, a thermosensitive liposomal doxorubicin is currently under clinical trials. [20, 13] Ultrasound triggered delivery is either arising from an increase of temperature when using thermosensitive liposomes,[21] or due to cavitation for non-thermosensitive liposomes.[22] However, the combination of temperature and cavitation enhances drug delivery for thermosensitive liposomes.[16] Polymer systems were also considered such as polymeric micelles,[23, 24] for which drug delivery is triggered by cavitation, and polymeric nanoparticles.[25, 26, 27] For the latter, nanoparticles made of a perfluorooctyl bromide (PFOB) core and a PLGA polymer shell coated with polyethylene glycol (PEG)[8] represent potential candidates to be used as theranostic agents[25, 26] in combination with MRI-g-HIFU technique. Indeed, these nanoparticles can be used as contrast agents for ^{19}F MRI [28, 8] while encapsulating a cytotoxic drug. Boissenot *et al.*[26] studied the drug delivery triggered by ultrasound from these systems and observed only a small drug delivery with no vaporization of the PFOB core. Luo *et al.*[27] used similar nanoparticles to successfully deliver drugs into glioblastoma cells implanted in mice using high intensity focused ultrasound (HIFU). In their case, a rapid and important release of doxorubicin is observed which, according to the authors, is induced by a vaporization of the PFOB liquid. In order to obtain a better understanding of the ultrasound triggered release from these types of nanoparticle, we have studied by spectrofluorometry the release of encapsulated Nile red using focused ultrasound for various ultrasonic properties. Nile red was chosen because it possesses an hydrophobicity similar to hydrophobic anticancer and non-fluorescent drugs such as paclitaxel or docetaxel, while exhibiting the advantage to be fluorescent only in hydrophobic environments as well as being less cytotoxic than drugs. We showed that it is indeed possible to release a large quantity of Nile red in a short time but only for specific ultrasonic parameters.

2. Experimental

Materials

Methylene chloride RPE-ACS 99.5% was provided by Carlo-Erba Reactifs (France). Sodium cholate (SC) and Nile red were purchased from Sigma-Aldrich (France). Poly (D,L-lactide-co-glycolide) – poly(ethylene glycol) (PLGA – PEG) Resomer RGP d 50105 (PLGA Mn = 45000 g/mol and 10 wt% of PEG Mn = 5000 g/mol, intrinsic viscosity 0.72 dl/g) were obtained from Boehringer-Ingelheim (Germany). Perfluorooctyl bromide (PFOB) was purchased from Fluorochem (United Kingdom). Water was purified using either a RIOS/Milli-Q system (Millipore, France) or a PURELAB Option-Q unit (ELGA LabWater).

Nanoparticle preparation

The formulation of nanoparticles was prepared using an emulsion-evaporation method where the emulsion is a single oil (methylene chloride) in water emulsion where PFOB, PLGA-PEG and Nile red are all miscible in methylene chloride.[8] The evaporation of methylene chloride leads to the formation of PLGA-PEG shell surrounding a PFOB core and solubilizing Nile red.[29] Specifically, 100 mg of PLGA-PEG was first dissolved into 3.9 ml of methylene chloride before adding 100 µl of a solution containing 60 µg/ml of Nile red in methylene chloride. After complete dissolution of the polymer, 60 µl of PFOB was added dropwise to the solution until complete miscibility. This organic phase was then emulsified into 20 ml of 1.5% sodium cholate (w/v) aqueous solution using a vortex for 1 min, followed by sonication at 30% of the maximum power for 1 min over ice using a vibrating metallic tip (Digital Sonifier 250, Branson). Methylene chloride was then evaporated under magnetic stirring at 300 rpm for about 3 h in a thermostated bath at 20°C. After evaporation, nanoparticles were filtered through a 0.45 µm PVDF membrane and then washed by an ultracentrifugation cycle of 1 h at 27,440 g and 4°C. The supernatant was discarded and the final pellet of nanoparticles was resuspended into fresh water. To determine the final concentration of nanoparticles in the suspension, small known volumes of the suspension were freeze-dried for 24 h using Alpha 1-2LD Plus apparatus (Christ), and weighed. In our experiments, all suspensions were prepared so that the nanoparticle concentration was equal to 0.25% (w/v).

Liposomes

We used Caelyx, a liposomal doxorubicin formulation made of 2 mg/ml of doxorubicin·HCl encapsulated inside liposomes. The liposome bilayer is made of N-(Methylpolyoxyethylene oxycarbonyl)-1,2-distearoyl-sn-glycero-3-phosphoethanola-mine sodium salt (MPEG-DSPE), fully hydrogenated soy phosphatidylcholine (HSPC), and cholesterol. The liposomal formulation was suspended in a 10 mM histidine buffer (pH 6.5) containing 300 mM of sucrose, giving a osmolality of 346 mOs/Kg, in order to equilibrate the osmolality between the medium inside and outside of liposomes. In our measurements, the initial liposomal suspension was diluted 500 times in the same histidine buffer containing sucrose.

Fluorescence

Fluorescence spectra were acquired using a spectrofluorometer (model FP8300 from Jasco). Fluorescence intensities were measured for suspensions containing either nanoparticles or liposomes.

For liposomes, the fluorescence signal coming from encapsulated doxorubicin is quenched due to the high concentration of doxorubicin into the liposome. An increase in fluorescence intensity is expected upon the release of doxorubicin and the percentage of released doxorubicin was determined using:

$$R_{dox} = \frac{I - I_{init}}{I_{100\%} - I_{init}} \times 100 \qquad (1)$$

where I_{init}, I, and $I_{100\%}$ are respectively the fluorescence intensities of the liposome suspension before insonation, 20 min after HIFU exposure, and after the addition of triton X100 (at a concentration of 20 µl/ml) which leads to the release of all doxorubicin. Fluorescence intensities were measured at an emission wavelength of $\lambda_{em} = 558$ nm using an excitation wavelength of $\lambda_{ex} = 475$ nm. The 20 min delay before fluorescence measurements was chosen to allow the samples, previously insonified at 37°C, to cool down to ambient temperature at which fluorescence spectra were performed.

For nanoparticle suspensions, the release of encapsulated Nile red is accompanied by a decrease in fluorescence intensity as Nile red looses its fluorescence property in water. Thus, fluorescence intensity provides this time the quantity of Nile red remaining encapsulated. Note that the concentration of Nile red inside the polymeric shell is low enough to avoid fluorescence quenching. A 100% release of Nile red corresponds to nanoparticles devoid of Nile red. Consequently, the percentage of released Nile red, R_{red}, was calculated using:

$$R_{red} = \left(1 - \frac{I - I_{void}}{I_{init} - I_{void}}\right) \times 100 \qquad (2)$$

where I_{void}, I_{init}, and I are respectively the fluorescence intensities of a suspension containing nanoparticles without any Nile red, of a suspension of nanoparticles containing Nile red at the beginning of the experiment, and at the end of experiment (i.e. 20 min after insonation or temperature incubation). Fluorescent intensities were measured at an emission wavelength of $\lambda_{em} = 575$ nm and an excitation wavelength of $\lambda_{ex} = 530$ nm.

Ultrasonic setup

The ultrasonic setup is schematically described in Fig. 1. Acoustic waves were generated by a focused transducer (Model H-101-G from Sonic Concepts), which input electrical signal came from a RF amplifier (model 150A100C from AR france) connected to the output of a waveform generator (model 33220A from Agilent). The acoustic wave propagated into a closed thermostated tank (at either $T_{tank} = 25$ or 37 ± 0.2°C) containing highly degassed water, thanks to a degassing machine (Model WDS-105 from Sonic Concepts) connected to the tank. A medical balloon (purchased from Nordson Medical), whose polyethylene terephthalate wall was 35 µm thick, was placed at the focus of the transducer so that the focal region (1.5 mm in diameter and 8 mm in length) lied inside the balloon. The balloon was filled with 2.5 ml of the solution to be studied and exhibited a tiny air/solution interface area ($\approx 1.3 - 2.3$ mm^2) at both ends. An ultrasonic absorber covered the lid of the tank as well as all its walls, except the one supporting the transducer, to avoid ultrasonic wave reflections inside the tank. Inertial cavitation occurring into the balloon solution was monitored using a focused broadband hydrophone (model Y-107 from Sonics Concepts). Tone bursts at 1.1 MHz with a 200 Hz pulse repetition frequency were used to sonicate samples. Typical sonication durations were 3 min for nanoparticle suspensions and 1 min 30 s for liposome suspensions, while duty cycle (from 5 to 50%) and acoustic pressure (up to 15.6 MPa) were varied to study the release behavior of both suspensions. A directional power sensor (model NAP-Z8 from Rohde & Schwarz), connected to a power reflection meter (Model NRT from Rohde & Schwarz), measured the average electrical power that was converted to an average acoustic power by the transducer. Finally, the acoustic peak-to-peak pressure P_{pkpk} at the transducer focus and the intensity I_{spta} (that is the spatial peak intensity averaged over the period of exposure at the focal point which surface section is 0.0177 cm^2) were derived from the average acoustic power. Absorption due to the balloon wall was neglected in those calculations as the balloon wall was very thin.

Finally, two temperature probes were used: a first one to measure T_{tank}, the temperature of the degassed water inside the tank, and a second one to record $T_{balloon}$, the temperature at the balloon outside surface. Note that the use of a hydrophone or a temperature probe inside the medical balloon was avoided as they will become the source of cavitation nuclei and bias the measurements.

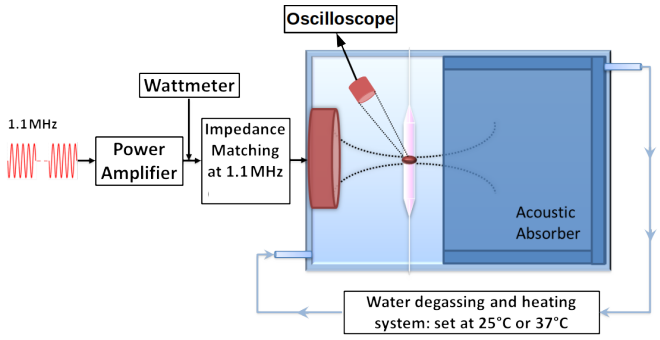

Figure 1: Scheme of the ultrasonic setup used to perform ultrasound-trigger drug release experiments.

Size measurements

Average hydrodynamic diameter (D) and polydispersity index (PDI) of nanoparticles were measured by dynamic light scattering at a scattering angle of 173° (using a Nano ZS from Malvern Instruments). The nanoparticle

suspensions were diluted in water and measured in triplicate at 25°C. Zeta potential measurements were determined with the same equipment, after a dilution in 1 mM NaCl at 25°C.

TEM measurements

Nanoparticles were observed by transmission electron microscopy (TEM) using a JEOL 1400 (Jeol Ltd, Japan) operating at 80 kV fitted with a SC1000 Orius camera (Gatan Inc, US). Copper grids coated with a formvar film were deposited on a 20 µl drop of nanoparticle suspension (0.05% (w/v) concentration) for 1 min and then on a 20 µl drop of phosphotungstic acid 2% solution for negative staining. The excess of liquid was then blotted off the grids using filter paper. Grids were observed the same day of preparation.

2.1. Lactic acid quantification

After the incubation or insonation of samples at 25 and 37°C, the amount of lactic acid was measured as previously detailed [30] in the supernatant of the centrifuged nanoparticle suspensions.

2.2. Statistics

All statistical analyses were performed using the JMP software (SAS Institute Inc., Cary, NC, USA). The statistical level of significance was set to $p = 0.05$. Scores were reported as means and standard deviation. Comparison of groups were performed with ANOVA, Chi-square tests or non-parametric Wilkoxon tests on ranks when necessary. Linear model was used to study relation between release rate or energy and experimental conditions. Logistic regression and ROC curves helped in defining the best threshold to separate high release rate (> 0.30) from moderate release rate (< 0.30) using AUC (Area Under Curve) and accuracy (proportion of cases correctly predicted).

3. Results

HIFU-triggered release of Nile red encapsulated in nanoparticles

The preparation of nanoparticles followed a reliable and proven protocol that ensured that all nanoparticles are composed of a PFOB liquid core and a PLGA-PEG shell encapsulating Nile red.[31, 25] The properties of these nanoparticles are also well defined,[8, 32] in particular their mean diameter is approximately equal to 140 nm while their polymeric shell is about 30 nm thick.[31] Insonation was performed for 3 min at a frequency of 1.1 MHz and a pulse repetition frequency of 200 Hz on suspensions (at a nanoparticle volume fraction of 0.25%) filling the medical balloon located inside the thermostated tank. Fluorescence intensities of the sample were recorded before and after insonation and were used to derive the amount, in percent, of released Nile red R_{red}. The values of R_{red} are plotted in Fig. 2 as a function of the total averaged acoustic energy applied at the transducer focus,[33] calculated by taking the spatial peak temporal average intensity I_{spta} times the time of insonation (i.e. $\tau = 3$ min). I_{spta} is often considered as an indicator of the ultrasonic thermal deposition. [33, 34] R_{red} values are also plotted in Fig. 3 as a function of P_{pkpk}, which is the acoustic parameter, in our experiments, that will lead to cavitation and modulate cavitation strength. In our conditions, the threshold for inertial cavitation occurrence was about 6.4 MPa, at which the focused hydrophone started to detect a characteristic signal made of a broadband background noise and harmonics. For some experiments, a temperature probe was kept in contact with the outside surface of the medical balloon during insonation, which provides $T_{balloon}$. In

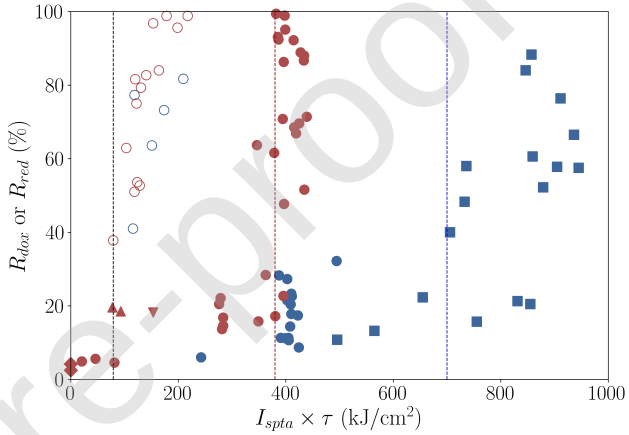

Figure 2: Percentage of released doxorubicin R_{dox} from liposomal doxorubicin at 25°C (○) and 37°C (○). Percentage of released Nile red from nanoparticles at 25°C (● and ■) and at 37°C (♦, ▼, ▲, and ●).In these measurements, the duty cycle was set either at 0 (♦), 5% (▲), 10% (▼), 25% (● and ●) or 50% (■). Vertical dashed lines are guides for eyes to indicate critical values of $I_{spta} \times \tau$ (see text): the black, red and blue lines are at 79, 380 and 700 J/cm^2. Note that while I_{spta} is expressed in W/cm^2, the unit of $I_{spta} \times \tau$ is J/cm^2. The latter allows to make comparison between measurements made at different insonation time τ.

Fig. 2 and 3, the experimental points exhibiting the same symbol and color correspond to similar conditions of insonation (identical DC and τ) and temperature (identical T_{tank}). Disparities can be observed due to differences in the nanoparticle formulations (e.g. in diameter and shell thickness) used in our experiments. Indeed, the behavior of the released points in Fig. 2 and 3 from the same batch and performed at different days exhibit a better reproducibility than when comparing released points from different batches. In Table 1, the temperature values at the balloon surface were averaged over several measurements, and the corresponding estimated P_{pkpk} range was given.

First measurements were conducted with a water tank thermostated at $T_{tank} = 37$°C. The results are shown as red symbols in Fig. 2 and 3 where the duty cycle (DC) was set at either 5 (▲), 10 (▼) or 25% (●). A weak release

($< 5\%$) of Nile red was measured below a total average intensity of $I_{spta} \times \tau = 79$ kJ/cm^2 ($I_{spta} \approx 0.44$ kW/cm^2) in Fig. 2 or below a peak-to-peak pressure of $P_{pkpk} = 6.4$ MPa in Fig. 3. Above these values, the Nile red release first increased at approximately 20%. Then, for a duty cycle of 25%, the values could further increase up to 100% for values of $I_{spta} \times \tau$ and P_{pkpk} that have been determined to be respectively 380 kJ/cm^2 ($I_{spta} \approx 1.5$ kW/cm^2, AUC= 0.85 and accuracy= 0.76) and 13 MPa (AUC= 0.86 and accuracy= 0.83). For $DC = 25\%$, the probe measured a rise in temperature from 37°C to 37.7, 44.3 and 45.7°C on the balloon surface during insonation when P_{pkpk} was equal to 6.2, 11.4–11.6 and 13.4–14.3 MPa, respectively (see Table 1). Whereas for $DC = 5\%$ a maximum temperature of 41.3°C was measured at the balloon surface when $P_{pkpk} = 13.1 - 13.9$ MPa. Similar experiments were performed with a water tank set at 25°C. Since duty cycles of 5 and 10% were previously inducing only a small Nile red release ($< 20\%$), only a DC of 25% was considered while keeping the other ultrasonic parameters the same as previously. The use of a 25% duty cycle did not lead to a high Nile red release (i.e. $> 35\%$) when $T_{tank} = 25$°C contrary to measurements made at $T_{tank} = 37$°C, as shown in Fig. 2 and 3, and this difference is significant ($p < 0.005$). However, we succeeded at achieving a higher release (i.e. $> 35\%$) by using a higher duty cycle of 50% but without reaching a 100% release. For DC = 50%, the best discriminating total average energy for having a high release rate is around 700 ($I_{spta} \approx 3.9$ kW/cm^2, AUC = 0.94 and accuracy = 0.88) while the best discriminating pressure is around 14 MPa (AUC = 0.79 and accuracy = 0.88). The temperature at the balloon surface was increasing from 25°C, before insonation, to 30.8 and 33.1°C at a duty cycle of 25% when P_{pkpk} was equal to 10.7 and 13.6-15.3 MPa, respectively and to 33.4 and 36.2°C at a duty cycle of 50% when P_{pkpk} was equal to 13.2 and 14.1-15.0 MPa, respectively.

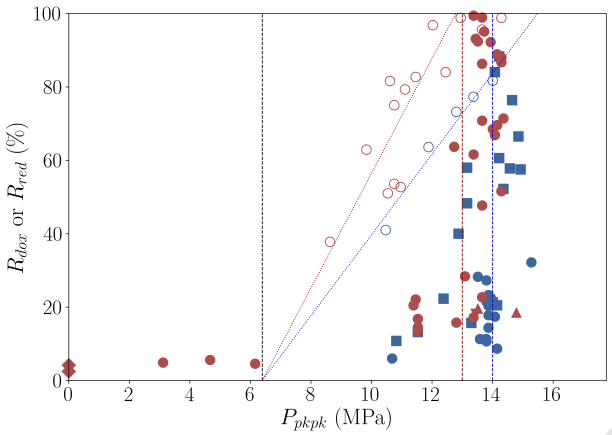

Figure 3: Percentage of released doxorubicin R_{dox} from liposomal doxorubicin at 25°C (○) and 37°C (○).Percentage of released Nile red from nanoparticles at 25°C (● and ■) and at 37°C (♦, ▼, ▲, and ●). In these measurements the duty cycle was set either at 0 (♦), 5% (▲), 10% (▼), 25% (● and ●) or 50% (■). Vertical dashed lines are guides for eyes to indicate critical values of P_{pkpk} (see text): the black, red and blue lines are at 6.4, 13 and 14 MPa.The dotted red and blue lines indicate the linear behavior expected for liposomal doxorubicin (starting around 6.4 MPa, at which strong inertial cavitation starts to occur).

T_{tank} (°C)	DC (%)	τ (min)	P_{pkpk} (MPa)	$T_{balloon}$ (±1.5°C)
37	5	3	13.1-13.7	41.3
	25	1	14.0-14.1	43.1
		2	13.7-15.3	46.6
		3	6.1	37.7
			11.4-11.5	44.3
			13.4-14.3	45.7
25	25	3	10.7	30.8
			13.5-15.3	33.1
		10	13.8	32.4
	50	3	13.1	33.4
			14.0-14.9	36.2

Table 1: The table displays the mean value of $T_{balloon}$ measured during insonation at the balloon outside surface, for various tank temperatures T_{tank}, duty cycles DC, insonation times τ, and peak pressures P_{pkpk}.

Overall, when considering $I_{spta} \times \tau$ as a linear model of the variables DC and T_{tank} ($R^2 = 0.79$), there is a significant influence of both duty cycle ($p < 0.0001$) and tank temperature ($p = 0.01$) to $I_{spta} \times \tau$, but with no significant interaction between them. This is also true when considering the release rate R_{red} as a linear model of DC and T_{tank} ($R^2 = 0.25$), with a significant influence of both DC ($p < 0.005$) and T_{tank} ($p < 0.0001$) but no significant interaction between them.

The insonation time of 3 min was chosen so that it was possible to reach 100% release of Nile red when using optimal parameters at 37°C. When decreasing the insonation times, while keeping a constant duty cycle of 25% and $P_{pkpk} \approx 13.4 - 14.1$ MPa, the amount of released Nile red was proportionally reduced as shown in Fig. 4. During the insonation, the temperature at the balloon surface was equal to 43.1, 46.6, and 45.7 ± 1.5°C at 1, 2 and 3 min (see Table 1). In the absence of insonation, nanoparticle suspensions kept 3 to 7 min at 37°C exhibited only a slight release of Nile red with $R_{red} \approx 2.7\%$.

Furthermore, we used TEM to monitor any change in nanoparticles morphologies induced by insonation at $T_{tank} = 25$°C and $DC = 50\%$, then at 37°C and 25%, by comparing non-insonified suspensions with samples insonified at low and high values of P_{pkpk}, as shown in Fig. 5. At both temperatures, we observed a few damaged nanoparticles after insonation only for high values of P_{pkpk} (≈ 14.5 MPa). We also measured in Fig. 6 the mean diameter of the nanoparticles before and after insonation, at 25 and 37°C. It did not vary significantively between the various samples, even is the mean diameter for samples insonified at $P_{pkpk} \approx 14.5$ MPa, is slightly higher than those observed without insonation or at $P_{pkpk} \approx 11.3$ MPa.

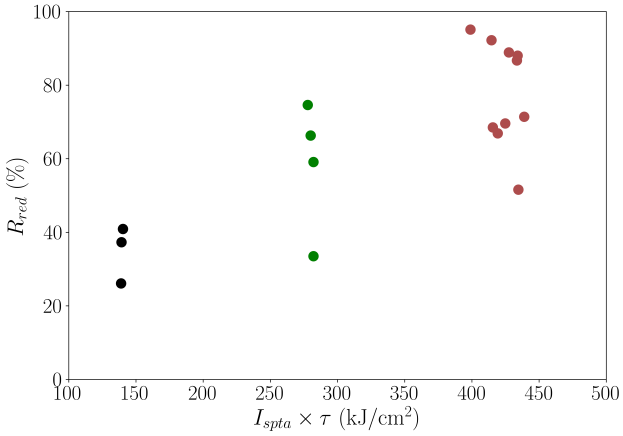

Figure 4: Variation in the percentage of released Nile red from nanoparticles using a constant value for I_{spta} but with a sonication time equals to 1 (●), 2 (●) or 3 min (●). Measurements were performed at 37°C with a 25% duty cycle and a P_{pkpk} in the range of 13.4–14.1 MPa.

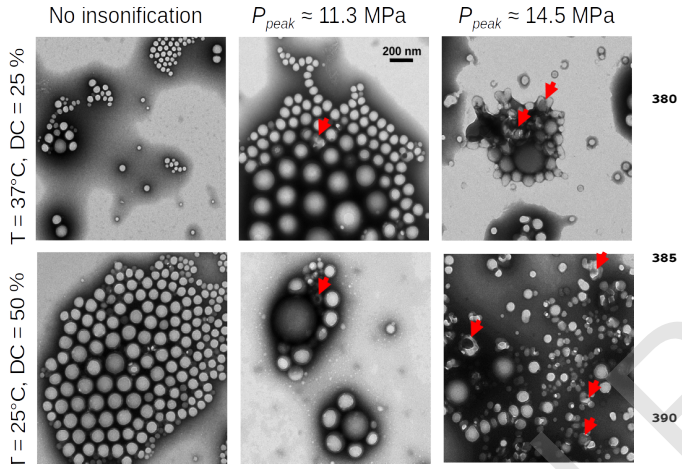

Figure 5: TEM pictures of nanoparticle solutions kept at 37°C (top row) without insonation (top left), insonified with a duty cycle of 25% at low (top middle) and high (top right) P_{pkpk} (resp. $I_{spta} \times \tau$) equal to 11.3 (resp. 279) and 14.3 MPa (resp. 434 kJ/cm^2), respectively. We respectively observed a 2.7, 22.1, and 88% release of Nile red. In the bottom row, TEM pictures are for nanoparticle solutions kept at 25°C without insonation (bottom left), insonified with a duty cycle of 50% at low (bottom middle) and high (bottom right) P_{pkpk} (resp. $I_{spta} \times \tau$) equal to 11.3 (resp. 566) and 14.6 MPa (resp. 912 kJ/cm^2), respectively. We respectively observed a 2.4, 13.2, and 76.4% release of Nile red. The scale bar is valid for all pictures. The red arrows indicate examples of damaged nanoparticles.

Finally, the amount of lactic acid was measured to $0.22 \pm 0.01\%$ and $0.17 \pm 0.01\%$ for samples incubated respectively at $T_{tank} = 25$ and 37°C. At 37°C, this amount remained constant at $0.17 \pm 0.01\%$ for samples insonified at $DC = 25\%$ and at $P_{pkpk} = 11.3$ or 14.3 MPa. Whereas at 25°C and $DC = 50\%$, the amount of lactic acid was measured to 0.21 ± 0.04 and 0.29 ± 0.08, respectively when $P_{pkpk} = 11.3$ and 14.6 MPa.

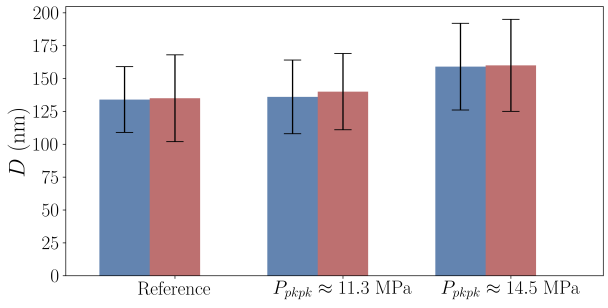

Figure 6: Diameter of polymeric nanoparticles were measured by DLS when they were not insonified (Reference), after an insonation with a medium P_{pkpk} (≈ 11.3 MPa) or a high P_{pkpk} (≈ 14.5 MPa), at 25°C with a 50 % duty cycle (blue bars) and 37°C with a 25% duty cycle (red bars).

HIFU-triggered release of doxorubicin encapsulated inside liposomes

We performed similar experiments using Caelyx, a liposomal form of doxorubicin·HCl. The mean diameter of Caelyx liposomes were measured by DLS and was equal 170 ± 20 nm in good agreement with the supplier specifications (mean size ranging from 160 to 180 nm) with a polydispersity index lower than 0.08. The initial liposomal suspension was diluted 500 times (to be in the same conditions as in the study of Somaglino *et al.*[35]) before being introduced into the balloon of the experimental setup. The solution was then insonified with the exactly same ultrasonic parameters as for polymeric nanoparticles except we only used a duty cycle of 25% and the time of insonation was set to 1 min 30 s. Indeed, when using a longer time of 3 min as was done previously we systematically reached a 100% doxorubicin release. A shorter time allowed us to vary the quantity of released doxorubicin as a function of P_{pkpk} or $I_{spta} \times \tau$. Insonation was performed with a water tank set at either $T_{tank} = 25$ or 37°C with a P_{pkpk} value varying from approximatively 8.5 to 14.1 Mpa, for which inertial cavitation was always detected by the hydrophone as it has already been shown that the doxorubicin release can be triggered by ultrasound only in presence of inertial cavitation [35, 16]. The amount of released doxorubicin from liposomes, R_{dox}, was recorded by fluorescence spectroscopy and the values are reported in Fig. 2 and 3. For both temperatures, we measured a continuous increase in doxorubicin release as $I_{spta} \times \tau$ or P_{pkpk} was increasing, reaching a maximum release at about 212 kJ/cm^2 and 12.7 MPa at 25°C, and at higher values (extrapolated to approximately 283 kJ/cm^2 and 15.6 MPa) at 37°C (see Fig. 2 and 3). The release rate was significantly different ($p < 0.005$) between doxorubicin-loaded liposomes and Nile red-loaded nanoparticles experiments at both 25°C and 37°C.

4. Discussion

Ultrasound are mechanical waves whose compression and depression induce a mechanical stress, they are also carrying energy that is dissipated through the medium in which ultrasound propagates, thus locally rising the temperature. When the acoustic pressure is high enough, cavitation occurs which further increases the local temperature and mechanical stress as well as creates radicals. In our case, cavitation started to be detected by the focused hydrophone when the peak-to-peak pressure P_{pkpk} was larger than 6.4 MPa. Published investigations showed that the ultrasound triggered doxorubicin release from the non-thermosensitive liposomal formulation caelyx is only due to inertial cavitation [35, 16]. Literature data [36, 37, 22, 21] show a linear behavior for the release from non-thermosensitive liposomal formulation as a function of acoustic pressure (or mechanical index), that starts at the critical pressure, P_{cav}, at which cavitation appears with a temperature dependant slope $\alpha(T)$: i.e. $R_{dox}(P) = \alpha(T)(P_{pkpk} - P_{cav})$. Here, the temperature dependence of α is not related to a gel-to-liquid transition (as the lipid membrane remains in a gel phase in these liposomal formulations) but to a change in water temperature-dependent properties [22, 38, 39]: in particular in the amount of gas dissolved in water (involved in nuclei appearance), in the surface tension at water/gas interface (involved in bubble stability), and in the vapor pressure, density and viscosity of water (involved in bubble volume oscillation and implosion). Moreover, Somaglino *et al.*[35] showed that the percentage of doxorubicin delivered from the liposomal formulation caelyx is proportional to the inertial cavitation dose. In our experiments, we also observed a linear behavior for the release of doxorubicin from caelyx as a function of P_{pkpk}. This indicates that when the value P_{pkpk} increases the inertial cavitation dose is also increasing, resulting in a higher doxorubicin release. However, this linear behavior is not observed for Nile red release from polymeric nanoparticles, suggesting a release mechanism that is not continuously proportional to the inertial cavitation dose. Nile red release occurs only for specific ultrasound properties, as below critical values of P_{pkpk} or $I_{spta} \times \tau$ only a low Nile red release was observed. Indeed, when considering Fig. 3, where R_{red} is plotted as a function of P_{pkpk}, the curves obtained at 25 and 37℃ follow the same behavior. A high Nile red release ($R_{nano} > 30\%$) is measured only for $P_{pkpk} > 13$ MPa. A moderate release $5\% < R_{nano} < 30\%$ is observed for $6.4 < P_{pkpk} < 13$ MPa, knowing that inertial cavitation occurs above 6.4 MPa in our setup, while only a low release is measured ($R_{nano} < 5\%$) in the absence of inertial cavitation (i.e. when $P_{pkpk} < 6.4$ MPa), similar to what is measured for non-insonified solutions. However, the above behavior is only observed for a duty cycle equals to 25% at 37℃ and 50% at 25℃. Indeed, a strong release ($> 30\%$) was never measured for $P_{pkpk} > 13$ MPa when the duty cycle was 5% or 10% at 37℃ or 25% at 25℃.

Meanwhile, the temperature measured at the balloon surface increases when the values of duty cycle and P_{pkpk} are increasing. For the same P_{pkpk} range (around 14.1 MPa), a similar temperature elevation is measured at 25% DC: +8.7℃ at 37℃ and +8.1 ℃ at 25℃, while the temperature elevation is +11.2℃ for a duty cycle of 50% at 25℃. At 5% DC and 37℃, the temperature elevation was about 4.1℃, twice less than for DC = 25%. Alternatively, for the same value of duty cycle (i.e 25%) the temperature $T_{balloon}$ decreases by about 2.3℃ when P_{pkpk} decreases from 13.5-15.3 to 10.7 MPa when $T_{tank} = 25$℃ (see Table 1). It should be noted that these temperature elevations can be higher at the focal point, inside the balloon. Given the definition of I_{spta}, its value increases for either increasing the value of duty cycle or acoustic pressure when all other ultrasonic parameters are kept constant. Since the local temperature increases when DC increases, I_{spta} effectively represents in our case a marker of the quantity of heat deposited from ultrasound at the focal zone. Consequently, the reason why the critical value of $I_{spta} \times \tau$ is larger at 25℃ than at 37℃ in Fig. 2 may come from the fact that more heat needs to be locally delivered by ultrasound at 25℃ than at 37℃ to induce a strong Nile red release.

Overall, our data suggest that the release of Nile red is triggered by a synergistic effect of temperature elevation and cavitation strength. Indeed, on one hand a high cavitation dose (that increases with P_{pkpk}) cannot alone induce a high delivery rate if the temperature at the focal region is not high enough. This is illustrated by the data performed above 13 MPa. A duty cycle of 25% can lead to 100% of Nile red release at $T_{tank} = 37$℃, while increasing the local temperature by 8.1℃ to reach 45.7℃. But at $T_{tank} = 25$℃, this value of duty cycle only promotes less than 30% of Nile red release for a similar temperature elevation of 8.7℃, which results in a temperature on the balloon surface of 33.1℃. Even an increase of duty cycle to 50% does not allow to reach 100% release, while the local temperature being 36.2℃. On the other hand, the sole temperature elevation cannot be held responsible for the observed high Nile red release, the application of a high dose of cavitation is required. Indeed, at 37℃ and in the absence of insonation, no change in the nanoparticle morphologies is observed and the passive release of Nile red (due to polymer shell hydrolysis combined with Nile red diffusion) always remains below 5% after 3 to 7 min of incubation (data points at 0 in Fig. 2 and 3), in agreement with other studies on similar polymer.[40] Note that in the latter case, the decrease in Nile red fluorescence intensity may partially originate from photobleaching. Moreover, the reason why a temperature rise is needed in addition to sufficient inertial cavitation cannot be explained by the glass transition temperature, T_g, of the polymeric shell since for the diblock polymer PLGA-PEG this value is equal to 27℃, a value obtained by differential scanning calorimetry.[31] This value is smaller than that of PLGA (around 40℃). It is also worth noting that T_g rapidly decreases due to polymer hydrolysis. For instance, the value

of T_g for PLGA nanoparticles goes below 20°C after several days of degradation.[40]

The fact that cavitation is required to induce a drug delivery from polymeric nanoparticles is consistent with the literature. For instance, Kost *et al.*[41] studied the ultrasound-triggered release of p-Nitroaniline encapsulated into various polymers, using an ultrasonic bath at 75 kHz. The authors observed that the release of p-Nitroaniline was drastically reduced when cavitation was minimized. Luo *et al.*[27] studied the ultrasound-triggered delivery of doxorubicin encapsulated inside PLGA-PEG nanoparticles with a diameter of 40 nm comprising a small amount of PFOB. The authors used their ultrasonic device at a power of 8.5–10.5 W but they did not provide pressure values nor the frequency used. They achieved *in vitro* an important ultrasound-triggered release (50–80%) that is accompanied, after insonation, with a large increase in particle size (up to 4 times), a decrease in zeta potential, and a change in droplet morphology that suggests the occurence of cavitation induced by PFOB vaporisation. However, Boissenot *et al.*[26] could not trigger a significant release of paclitaxel encapsulated in the same nanoparticles used in our study, although cavitation occured during insonation. The authors used a maximum peak negative pressures of 7 MPa with a duty cycle of 20% (at 37°C), which values may not be sufficient to obtain a high release in regard to our results. That may also be the case for Abed *et al.*[42] who could never induce a release of 5-fluorouracil larger than 6% at 37°C (measured just after insonation) when encapsulated into nanoparticles made of a PLGA shell and encapsulating a small magnetite core. Indeed, the authors used small ultrasonic intensities (< 1 W/cm^2) at a frequency of 3 MHz.

In our experiments, after high pressure insonation, we observed no significant change in particle size and no dramatic structural modifications of the nanoparticles as those measured by Luo *et al.* after PFOB vaporization, and our acoustic spectra exhibit no evidence of PFOB vaporization. The difference may come from the nanoparticles size and from the fact that our nanoparticles contain a well defined PFOB core representing approximately 30% of the nanoparticle volume whereas for the nanoparticles of Luo *et al.*, the quantity of PFOB represents only 1% of the droplet weight and may be distributed in several locations into the nanoparticle. PFOB is known to solubilize important quantity of oxygen (20 times more than water)[43] which can favor PFOB vaporization. But in our case, the presence of a thick polymer shell strongly acts against an expansion of the PFOB volume. However, it has been shown that the quantity of oxygen solubilized in perfluorocarbons varies with temperature and it increases in the case of PFOB[44] while it decreases for water when the temperature rises. This variation should induce a migration of oxygens from water to PFOB, through the polymer, thus enriching the polymer with oxygen. Considering this fact, we hypothesize for the nanoparticles studied here that when P_{pkpk} is large enough, the increase in R_{red} from 3 to 20% observed for $P_{pkpk} < 13$ MPa is due to a degradation of the polymer shell surface induced by the cavitation occuring in the aqueous solvent surrounding the nanoparticles. While for $P_{pkpk} > 13$ MPa, cavitation may also occur inside the polymer shell if the temperature is large enough to enrich the shell with oxygen due to its transfer from water to PFOB. This internal degradation should allow a larger diffusion of Nile red out of the polymer. This hypothesis offers the advantage to take into account the fact that both a high acoustic pressure and sufficient temperature elevation are required to induce a high Nile red release, while either a high acoustic pressure or a temperature elevation are not sufficient alone to induce this high release. However, more investigations are needed to validate this hypothesis. Future investigations should focus on the monitoring of oxygen inside the nanoparticles as a function of temperature. ^{19}F MRI could be used for such studies although the required acquisition time will prevent a dynamic monitoring of oxygenation.[45]

Finally, considering the required values of pressure and duty cycle as well as the fact that strong inertial cavitation is needed to induce Nile red release, these nanoparticles are not suitable for therapeutic applications using ultrasound-triggered drug delivery.

5. Conclusion

We have investigated the ultrasound triggered release of Nile red encapsulated into nanoparticles made of a PLGA-PEG shell surrounding a PFOB core. We could induce an important release (>30%) of Nile red only if the pressure and temperature were high enough (i.e. $P_{pkpk} > 13$ MPa and $T > 45$°C). Otherwise, moderate release is obtained but only in the presence of inertial cavitation. Thus, these ultrasonic parameters make these nanoparticles unsuitable for therapies using ultrasound-triggered drug release.

6. acknowledgement

This work is supported by public grant ANR-10-NANO-06 overseen by the French National Research Agency (ANR) as part of the "Investissements d'Avenir" program and by the european program EuroNanoMed II (project SonoTherag). The present work has benefited from the facilities and expertise of the Electron Micoscopy facilities of Imagerie-Gif (http://www.i2bc.paris-saclay.fr/spip.php?article282) with the precious help of C. Boulogne. This core facility is member of the Infrastructures en Biologie Santé et Agronomie (IBiSA), and is supported by the French national Research Agency under Investments for the Future programs "France-BioImaging", and the Labex "Saclay Plant Science" (ANR-10-INSB-04-01 and ANR-11-IDEX-0003-02, respectively). Institut Galien Paris-Saclay is a member of the Laboratory of Excellence LERMIT supported by a grant from ANR (ANR-10-LABX-33). The authors also thank Domingues Gonçalves for building the ultrasonic tank used in this study.

[1] E. Fattal, N. Tsapis, Nanomedicine technology: current achievements and new trends, Clin. Transl. Imaging 2 (1) (2014) 77–87. doi:10.1007/s40336-014-0053-3.

[2] J. A. Sparano, A. N. Makhson, V. F. Semiglazov, S. A. Tjulandin, O. I. Balashova, I. N. Bondarenko, N. V. Bogdanova, G. M. Manikhas, G. P. Oliynychenko, V. A. Chatikhine, S. H Zhuang, L. Xiu, Z. Yuan, W. R. Rackoff, Pegylated liposomal doxorubicin plus docetaxel significantly improves time to progression without additive cardiotoxicity compared with docetaxel monotherapy in patients with advanced breast cancer previously treated with neoadjuvant-adjuvant anthracycline therapy: Results from a randomized phase iii study, J. Clin. Oncol. 27 (27) (2009) 4522–4529. doi:10.1200/JCO.2008.20.5013.

[3] S. Stewart, H. Jablonowski, F. D. Goebel, K. Arasteh, M. Spittle, A. Rios, D. Aboulafia, J. Galleshaw, B. J. Dezube, Randomized comparative trial of pegylated liposomal doxorubicin versus bleomycin and vincristine in the treatment of aids-related kaposi's sarcoma. international pegylated liposomal doxorubicin study group, J. Clin. Oncol. 16 (2) (1998) 683–91.

[4] H. Maeda, The enhanced permeability and retention (epr) effect in tumor vasculature: the key role of tumor-selective macromolecular drug targeting, Adv. Enzyme Regul. 41 (1) (2001) 189–207. doi:10.1016/S0065-2571(00)00013-3.

[5] H. Maeda, H. Nakamura, J. Fang, The EPR effect for macromolecular drug delivery to solid tumors: Improvement of tumor uptake, lowering of systemic toxicity, and distinct tumor imaging in vivo, Adv. Drug Delivery Rev. 65 (1) (2013) 71–79. doi:10.1016/j.addr.2012.10.002.

[6] H. Maeda, T. Sawa, T. Konno, Mechanism of tumor-targeted delivery of macromolecular drugs, including the EPR effect in solid tumor and clinical overview of the prototype polymeric drug SMANCS, J. Contr. Release 74 (1–3) (2001) 47–61. doi:10.1016/S0168-3659(01)00309-1.

[7] D. C. Drummond, O. Meyer, K. Hong, D. B. Kirpotin, D. Papahadjopoulos, Optimizing liposomes for delivery of chemotherapeutic agents to solid tumors, Pharmacol. Rev. 51 (4) (1999) 691–744.

[8] O. Diou, N. Tsapis, C. Giraudeau, J. Valette, C. Gueutin, F. Bourasset, S. Zanna, C. Vauthier, E. Fattal, Long-circulating perfluorooctyl bromide nanocapsules for tumor imaging by ^{19}FMRI, Biomaterials 33 (22) (2012) 5593–5602. doi:10.1016/j.biomaterials.2012.04.037.

[9] D. J. A. Crommelin, A. T. Florence, Towards more effective advanced drug delivery systems, Int. J. Pharm. 454 (1) (2013) 496–511. doi:10.1016/j.ijpharm.2013.02.020.

[10] S. Mura, J. Nicolas, P. Couvreur, Stimuli-responsive nanocarriers for drug delivery, Nature Materials 12 (11) (2013) 991–1003. doi:10.1038/nmat3776.

[11] J. Yao, J. Feng, J. Chen, External-stimuli responsive systems for cancer theranostic, Asian J. Pharm. Sci. 11 (5) (2016) 585–595. doi:10.1016/j.ajps.2016.06.001.

[12] S. Ganta, H. Devalapally, A. Shahiwala, M. Amiji, A review of stimuli-responsive nanocarriers for drug and gene delivery, J. Control. Release 126 (2008) 187–204. doi:10.1016/j.jconrel.2007.12.017.

[13] T. Boissenot, A. Bordat, E. Fattal, N. Tsapis, Ultrasound-triggered drug delivery for cancer treatment using drug delivery systems: From theoretical considerations to practical applications, J. Control. Release 241 (2016) 144–163. doi:10.1016/j.jconrel.2016.09.026.

[14] N. A. Clark, N. A. Clark, S. L. Mumford, J. H. Segars, Reproductive impact of mri-guided focused ultrasound surgery for fibroids: a systematic review of the evidence, Curr. Opin. Obstet. Gynecol. 26 (3) (2014) 151–161. doi:10.1097/GCO.0000000000000070.

[15] F. A. Jolesz, Mri-guided focused ultrasound surgery, Annu Rev. Med. 60 (2009) 417–430. doi:10.1146/annurev.med.60.041707.170303.

[16] S. Dromi, V. Frenkel, A. Luk, B. Traughber, M. Angstadt, M. Bur, J. Poff, J. Xie, S. K. Libutti, K. C. P. Li, B. J. Wood, Pulsed-high intensity focused ultrasound and low temperature-sensitive liposomes for enhanced targeted drug delivery and antitumor effect, Clin. Cancer Res. 13 (9) (2007) 2722–2727. doi:10.1158/1078-0432.CCR-06-2443.

[17] W. G. Pitt, G. A. Husseini, B. L. Roeder, D. Dickinson, D. Warden, J. Hartley, P. Jones, Preliminary Results of Combining Low Frequency Low Intensity Ultrasound and Liposomal Drug Delivery to Treat Tumors in Rats, J. Nanosci. Nanotechnol. 10 (2010) 1–5. doi:10.1166/jnn.2010.3117.

[18] S. Eggen, M. Afadzi, E. A. Nilssen, S. B. Haugstad, B. Angelsen, C. de L. Davies, Ultrasound improves the uptake and distribution of liposomal doxorubicin in prostate cancer xenografts, Ultrasound in Med. & Biol. 39 (7) (2013) 1255–1266. doi:10.1016/j.ultrasmedbio.2013.02.010.

[19] J.-L. Mestas, R. A. Fowler, T. J. Evjen, L. Somaglino, A. Moussatov, J. Ngo, S. Chesnais, S. Røgnvaldsson, S. L. Fossheim, E. A. Nilssen, C. Lafon, Therapeutic efficacy of the combination of doxorubicin-loaded liposomes with inertial cavitation generated by confocal ultrasound in AT2 Dunning rat tumour model, J. Drug Target. 22 (8) (2014) 688–697. doi:10.3109/1061186X.2014.906604.

[20] R. T. P. Poon, N. Borys, Lyso-thermosensitive liposomal doxorubicin: an adjuvant to increase the cure rate of radiofrequency ablation in liver cancer, Future Oncology 7 (8) (2011) 937–945. doi:doi:10.2217/fon.11.73.

[21] J.-M. Escoffre, A. Novell, M. de Smet, A. Bouakaz, Focused ultrasound mediated drug delivery from temperature-sensitive liposomes: in-vitro characterization and validation, Phys. Med. Biol. 58 (2013) 8153–8151. doi:10.1088/0031-9155/58/22/8135.

[22] M. Afadzi, C. de L. Davies, Y. H. Hansen, T. Johansen, Ø. K. Standal, R. Hansen, S.-E. Måsøy, E. A. Nilssen, B. Angelsen, Effect of ultrasound parameters on the release of liposomal calcein, Ultrasound in Med. & Biol 38 (3) (2012) 476–486. doi:10.1016/j.ultrasmedbio.2011.11.017.

[23] G. A. Husseini, G. D. Myrup, W. G. Pitt, D. A. Christensen, N. Y. Rapoport, Factors affecting acoustically triggered release of drugs from polymeric micelles, J. Control. Release 69 (1) (2000) 43–52. doi:10.1016/S0168-3659(00)00278-9.

[24] A. Marin, H. Sun, G. A. Husseini, W. G. Pitt, D. A. Christensen, N. Y. Rapoport, Drug delivery in pluronic micelles: effect of high-frequency ultrasound on drug release from micelles and intracellular uptake, J. Control. Release 84 (1–2) (2002) 39–47. doi:10.1016/S0168-3659(02)00262-6.

[25] T. Boissenot, E. Fattal, A. Bordat, S. Houvenagel, J. Valette, H. Chacun, C. Gueutin, N. Tsapis, Paclitaxel-loaded {PEGylated} nanocapsules of perfluorooctyl bromide as theranostic agents, Eur. J. Pharm. Biopharm. 108 (2016) 136–144. doi:10.1016/j.ejpb.2016.08.017.

[26] T. Boissenot, A. Bordat, B. Larrat, M. Varna, H. Chacun, A. Paci, V. Poinsignon, E. Fattal, N. Tsapis, Ultrasound-induced mild hyperthermia improves the anticancer efficacy of both taxol® and paclitaxel-loaded nanocapsules, Journal of Controlled Release 264 (2017) 219–227. doi:10.1016/j.jconrel.2017.08.041.

[27] Z. Luo, K. Jin, Q. Pang, S. Shen, Z. Yan, T. Jiang, X. Zhu, L. Yu, Z. Pang, X. Jiang, On-demand drug release from dual-targeting small nanoparticles triggered by high-intensity focused ultrasound enhanced glioblastoma-targeting therapy, ACS Appl. Mat. Int. 9 (37) (2017) 31612–31625. doi:10.1021/acsami.7b10866.

[28] E. Pisani, N. Tsapis, B. Galaz, M. Santin, R. Berti, N. Taulier, E. Kurtisovski, O. Lucidarme, M. Ourevitch, B. T. Doan, J.-C. Beloeil, B. Gillet, W. Urbach, S. L. Bridal, E. Fattal, Perfluorooctyl Bromide Polymeric Capsules as Dual Contrast Agents for Ultrasonography and Magnetic Resonance Imaging, Adv. Funct. Mat. 18 (19) (2008) 2963–2971. doi:10.1002/adfm.200800454.

[29] E. Pisani, E. Fattal, J. Paris, C. Ringard, V. Rosilio, N. Tsapis, Surfactant dependent morphology of polymeric capsules of perfluorooctyl bromide: Influence of polymer adsorption at the dichloromethane–water interface, J. Coll. Int. Sci. 326 (1) (2008)

66–71. doi:10.1016/j.jcis.2008.07.013.

[30] E. Pisani, N. Tsapis, J. Paris, V. Nicolas, L. Cattel, E. Fattal, Polymeric nano/microcapsules of liquid perfluorocarbons for ultrasonic imaging: Physical characterization, Langmuir 22 (9) (2006) 4397–4402. doi:10.1021/la0601455.

[31] O. Diou, A. Brûlet, G. Pehau-Arnaudet, E. Morvan, R. Berti, K. Astafyeva, N. Taulier, E. Fattal, N. Tsapis, Pegylated nanocapsules of perfluorooctyl bromide: mechanism of formation, influence of polymer concentration on morphology, and mechanical properties, Colloids Surf. B 146 (2016) 762–769. doi:10.1016/j.colsurfb.2016.07.033.

[32] K. Astafyeva, J.-L. Thomas, F. Coulouvrat, M. Guédra, O. Diou, L. Mousnier, N. Tsapis, W. Urbach, N. Taulier, Properties of theranostic nanoparticles determined in suspension by ultrasonic spectroscopy, Phys. chem. Chem. Phys. 17 (2015) 25483–25493. doi:10.1039/c5cp04424c.

[33] K. I. Carnes, J. L. Drewniak, F. Dunn, In utero measurements of ultrasonically induced fetal mouse temperature increases, Ultrasound Med. Biol. 17 (4) (1991) 373–382.

[34] R. L. King, Y. Liu, G. R. Harris, Quantification of temperature rise within the lens of the porcine eye caused by ultrasound insonation, Ultrasound Med. Biol. 43 (2) (2017) 476–481. doi:10.1016/j.ultrasmedbio.2016.09.021.

[35] L. Somaglino, G. Bouchoux, J.-L. Mestas, C. Lafon, Validation of an acoustic cavitation dose with hydroxyl radical production generated by inertial cavitation in pulsed mode: Application to in vitro drug release from liposomes, Ultrason. Sonochem. 18 (2011) 577–588. doi:10.1016/j.ultsonch.2010.07.009.

[36] A. Schroeder, Y. Avnir, S. Weisman, Y. Najajreh, A. Gabizon, Y. Talmon, J. Kost, Y. Barenholz, Controlling Liposomal Drug Release with Low Frequency Ultrasound: Mechanism and Feasibility, Langmuir 23 (7) (2007) 4019–4025. doi:10.1021/la0631668.

[37] Y. Hansen, C. d. L. Davies, M. Afadzi, B. Angelsen, T. Johansen, E. Nilssen, Ultrasonic drug release: impact on liposomal doxorubicin in collagens gels, in: IEEE Int. Ultr. Symp. Proc., IEEE, 2012, pp. 425–428. doi:10.1109/ULTSYM.2012.0105.

[38] R. E. Apfel, C. K. Holland, Gauging the likelihood of cavitation from short-pulse, low-duty cycle diagnostic ultrasound, Ultrasound Med. Biol. 17 (2) (1991) 179–185. doi:10.1016/0301-5629(91)90125-G.

[39] E. D. Bel, C. Janssen, S. D. Smet, H. V. Langenhove, J. Dewulf, Sonolysis of ciprofloxacin in aqueous solution: Influence of operational parameters, Ultrason. Sonochem. 18 (1) (2011) 184–189. doi:10.1016/j.ultsonch.2010.05.003.

[40] K. Elkharraz, N. Faisant, C. Guse, F. Siepmann, B. Arica-Yegin, J. M. Oger, R. Gust, A. Goepferich, J. P. Benoit, J. Siepmann, Paclitaxel-loaded microparticles and implants for the treatment of brain cancer: Preparation and physicochemical characterization, Int. J. Pharm. 314 (2006) 127–136. doi:10.1016/j.ijpharm.2005.07.028.

[41] J. Kost, K. Leong, R. Langer, Ultrasound-enhanced polymer degradation and release of incorporated substances, Proc. Natl. Acad. Sci. U.S.A. 86 (20) (1989) 7663–7666.

[42] Z. Abed, J. Beik, S. Khoee, S. Khoei, A. Shakeri-Zadeh, M. B. Shiran, Effects of ultrasound irradiation on the release profile of 5-fluorouracil from magnetic polylactic co-glycolic acid nanocapsules, J. Biomed. Phys. Eng. 6 (3) (2016) 183–194.

[43] K. C. Lowe, M. R. Davey, J. B. Power, Perfluorochemicals: their applications and benefits to cell culture, Trends Biotechnol. 16 (6) (1998) 272–277. doi:10.1016/S0167-7799(98)01205-0.

[44] J. L. H. Johnson, M. C. Dolezal, A. Kerschen, T. O. Matsunaga, E. C. Unger, In vitro comparison of dodecafluoropentane (ddfp), perfluorodecalin (pfd), and perfluoroctylbromide (pfob) in the facilitation of oxygen exchange, Artif. Cells Blood Substit. Biotechnol. 37 (4) (2009) 156–162. doi:10.1080/10731190903043192.

[45] O. Lorton, J.-N. Hyacinthe, S. Desgranges, L. Gui, A. Klauser, Z. Celicanin, L. A. Crowe, F. Lazeyras, E. Allémann, N. Taulier, C. Contino-Pépin, R. Salomir, Molecular oxygen loading in candidate theranostic droplets stabilized with biocompatible fluorinated surfactants: Particle size effect and application to in situ 19f mri mapping of oxygen partial pressure, J. Magn. Reson. 295 (2018) 27–37. doi:10.1016/j.jmr.2018.07.019.